Transient dynamics for sequence processing neural networks

Masaki KAWAMURA

Faculty of Science, Yamaguchi University,

Yoshida 1677-1, Yamaguchi, 753-8512 Japan[*]

Masato OKADA

RIKEN BSI, Wako-shi, 351-0198 Japan

(Dated: February 1, 2008)

Abstract

An exact solution of the transient dynamics for a sequential associative memory model is discussed through both the path-integral method and the statistical neurodynamics. Although the path-integral method has the ability to give an exact solution of the transient dynamics, only stationary properties have been discussed for the sequential associative memory. We have succeeded in deriving an exact macroscopic description of the transient dynamics by analyzing the correlation of crosstalk noise. Surprisingly, the order parameter equations of this exact solution are completely equivalent to those of the statistical neurodynamics, which is an approximation theory that assumes crosstalk noise to obey the Gaussian distribution. In order to examine our theoretical findings, we numerically obtain cumulants of the crosstalk noise. We verify that the third- and fourth-order cumulants are equal to zero, and that the crosstalk noise is normally distributed even in the non-retrieval case. We show that the results obtained by our theory agree with those obtained by computer simulations. We have also found that the macroscopic unstable state completely coincides with the separatrix.

[*]Electronic address: kawamura@sci.yamaguchi-u.ac.jp

I. INTRODUCTION

Statistical mechanical theories have been applied to the field of neural networks such as combinatorial optimization and associative memories. Recently, they have also been applied to the field of information science such as error-correcting codes, image recovery, and CDMA [1, 2, 3, 4, 5, 6, 7, 8]. For example, the maximum *a posteriori* probability (MAP) and the maximum posterior marginals (MPM) in the framework of the Bayesian estimation correspond to finding the ground state and the equilibrium state of the corresponding spin system, respectively. From this point of view, information processing can be treated as some kind of relaxation process of spin systems. The transient dynamics of systems should therefore be discussed from the information theoretic point of view.

In general, however, theoretical treatment of the dynamics is extremely difficult compared with the equilibrium statistical mechanics of frustrated systems into which many problems concerning the information processing are mapped. Although a lot of works has been done to analyze the transient dynamics [9, 10, 11], it is well known that achieving the tractable rigorous treatment is hopeless regarding the dynamics of frustrated systems. In this paper, we discuss a correlation type associative memory model having frustrated couplings, and rigorously derive an exact macroscopic description of the transient dynamics for this model.

There are two types of associative memory models: autoassociative memory models and sequential associative memory models. In the case of autoassociative memory models [12], their storage capacity and phase diagram have been analyzed by equilibrium theories [13, 14]. In the case of sequential associative memory models, there is no equilibrium state, since the network retrieves different patterns sequentially. As we mentioned above, since associative memory models definitely belong to information processing systems, it is important to analyze the information process, that is, the retrieval process of the stored patterns. Although the path-integral method based on the generating function [9, 15, 16, 17] has the potential ability to provide a rigorous solution for an associative memory model, the theory is formal and intractable because the complexity of the numerical calculation is exponentially large with respect to the time step. Accordingly, the theory can only describe the short time region and equilibrium state.

Recently, Düring et al. [18] presented the path-integral method regarding a sequential associative memory model. However, they did not discuss the transient properties of

the retrieval process, but only analyzed properties of the stationary state, i.e., the storage capacity and the phase diagram [18]. On the other hand, the statistical neurodynamics [10, 19, 20, 21, 22] is an approximation theory capable of analyzing the long-term behavior of the transient dynamics. Here, the input to the spin or neuron can be divided into two terms. The first one is a signal term, which is a signal to retrieve, and the second one is a crosstalk noise term, which prevents retrieval. In the statistical neurodynamics, one assumes that the crosstalk noise obeys the Gaussian distribution with mean 0 and a time dependent variance, and derives macroscopic recursive equations for the amplitude of the signal term and the variance of the crosstalk noise. Therefore, the basin of attraction and other dynamic properties can be discussed through the statistical neurodynamics. For the autoassociative memory model, Nishimori and Ozeki tried to numerically check the Gaussian assumption using large-scale computer simulations, and found that the assumption holds only when the retrieval process succeeds [20, 23].

In this paper, we derive an exact solution of the transient dynamics for the sequential associative memory model through the path-integral method, and derive an approximated solution through the statistical neurodynamics. We then compare the results of the two theories, and try to clarify their relationship.

This paper is constructed as follows. In the second section, the sequential associative memory model that we use is defined. In the third section, we introduce the formal macroscopic state equations obtained by Düring et al. using the path-integral method. In the fourth section, we derive an exact macroscopic description of the transient dynamics by the path-integral method. In the fifth section, we also derive macroscopic state equations by the statistical neurodynamics, and prove that both the path-integral method and the statistical neurodynamics give the same equations for the sequential associative memory model. In the sixth section, the transient dynamics are verified by comparing these theories with computer simulations.

II.   SEQUENCE PROCESSING NEURAL NETWORK

Let us consider a sequential associative memory model that consists of N spins or neurons. We consider the case of $N \rightarrow \infty$. The state of the spins takes $\sigma_i(t) = \pm 1$ and updates the

state synchronously with the following probability:

$$\text{Prob}\left[\sigma_i(t+1)|h_i(t)\right] \;=\; \frac{1}{2}\left[1 + \sigma_i(t+1)\tanh\beta h_i(t)\right], \tag{1}$$

$$h_i(t) \;=\; \sum_{j=1}^{N} J_{ij}\sigma_j(t) + \theta_i(t), \tag{2}$$

where β is the inverse temperature, $\beta = 1/T$. When the temperature is absolute zero, i.e., $T = 0$, the state of the spins $\sigma_i(t+1)$ is determined by the sign of local field $h_i(t)$, that is,

$$\sigma_i(t+1) = \text{sgn}\left[h_i(t)\right]. \tag{3}$$

The term $\theta_i(t)$ is a threshold or an external input to the network. Synaptic connection J_{ij} stores p random patterns $\boldsymbol{\xi}^\mu = (\xi_1^\mu, \cdots, \xi_N^\mu)^T$ so as to retrieve the patterns as $\boldsymbol{\xi}^1 \to \boldsymbol{\xi}^2 \to \cdots \boldsymbol{\xi}^p \to \boldsymbol{\xi}^1$ sequentially. For instance, it is given by

$$J_{ij} = \frac{1}{N}\sum_{\mu=1}^{p} \xi_i^{\mu+1}\xi_j^\mu, \tag{4}$$

where $\boldsymbol{\xi}^{p+1} = \boldsymbol{\xi}^1$. The number of stored patterns p is given by $p = \alpha N$, where α is called *the loading rate*. Each component of the patterns is assumed to be an independent random variable that takes a value of either $+1$ or -1 according to the following probability,

$$\text{Prob}\left[\xi_i^\mu = \pm 1\right] = \frac{1}{2}. \tag{5}$$

We determine the initial state $\boldsymbol{\sigma}(0)$ according to the following probability distribution,

$$\text{Prob}[\sigma_i(0) = \pm 1] = \frac{1 \pm m(0)\xi_i^p}{2}, \tag{6}$$

and therefore the overlap between the pattern $\boldsymbol{\xi}^p$ and the initial state $\boldsymbol{\sigma}(0)$ is $m(0)$. The network state $\boldsymbol{\sigma}(t)$ at time t is expected to be near the pattern $\boldsymbol{\xi}^t$, when initial overlap $m(0)$ is large and the loading rate is small.

III.   PATH-INTEGRAL METHOD

Düring et al. [18] discussed the sequential associative memory model by the path-integral method. In this section, we introduce macroscopic state equations for the model with a finite temperature $T \geq 0$, according to their paper. The detailed derivation is available in their paper [18].

In order to analyze the transient dynamics, the generating function $Z[\boldsymbol{\psi}]$ is defined as

$$Z[\boldsymbol{\psi}] = \sum_{\boldsymbol{\sigma}(0),\cdots,\boldsymbol{\sigma}(t)} p\left[\boldsymbol{\sigma}(0), \boldsymbol{\sigma}(1), \cdots, \boldsymbol{\sigma}(t)\right] e^{-i\sum_{s<t} \boldsymbol{\sigma}(s)\cdot\boldsymbol{\psi}(s)}, \tag{7}$$

where $\boldsymbol{\psi} = (\boldsymbol{\psi}(0), \cdots, \boldsymbol{\psi}(t-1))$. The state $\boldsymbol{\sigma}(s) = (\sigma_1(s), \cdots, \sigma_N(s))^T$ denotes the state of the spins at time s, and the probability $p\left[\boldsymbol{\sigma}(0), \boldsymbol{\sigma}(1), \cdots, \boldsymbol{\sigma}(t)\right]$ denotes the probability of taking the path from initial state $\boldsymbol{\sigma}(0)$ to state $\boldsymbol{\sigma}(t)$ at time t through $\boldsymbol{\sigma}(1), \boldsymbol{\sigma}(2), \cdots, \boldsymbol{\sigma}(t-1)$. As (7) shows, the generating function takes the summation of all $2^{N(t+1)}$ paths, which the network can take from time 0 to t. The generating function $Z[\boldsymbol{\psi}]$ involves the sequence overlap $m(s)$, which represents the direction cosine between the state $\boldsymbol{\sigma}(s)$ and the retrieval pattern $\boldsymbol{\xi}^s$ at time s, the response functions $G(s, s')$, and the correlation functions $C(s, s')$ as follows:

$$m(s) = i \lim_{\boldsymbol{\psi}\to 0} \frac{1}{N} \sum_{i=1}^N \xi_i^s \frac{\partial Z[\boldsymbol{\psi}]}{\partial \psi_i(s)} = \frac{1}{N} \sum_{i=1}^N \xi_i^s \left\langle \sigma_i(s) \right\rangle, \tag{8}$$

$$G(s, s') = i \lim_{\boldsymbol{\psi}\to 0} \frac{1}{N} \sum_{i=1}^N \frac{\partial^2 Z[\boldsymbol{\psi}]}{\partial \psi_i(s)\partial \theta_i(s')} = \frac{1}{N} \sum_{i=1}^N \frac{\partial \left\langle \sigma_i(s) \right\rangle}{\partial \theta_i(s')}, \tag{9}$$

$$C(s, s') = - \lim_{\boldsymbol{\psi}\to 0} \frac{1}{N} \sum_{i=1}^N \frac{\partial^2 Z[\boldsymbol{\psi}]}{\partial \psi_i(s)\partial \psi_i(s')} = \frac{1}{N} \sum_{i=1}^N \left\langle \sigma_i(s)\sigma_i(s') \right\rangle, \tag{10}$$

where $\langle \cdot \rangle$ denotes the thermal average. Using the assumption of self-averaging, we replace the generating function $Z[\boldsymbol{\psi}]$ with its ensemble average $\overline{Z}[\boldsymbol{\psi}]$.

Evaluating the averaged generating function $\overline{Z}[\boldsymbol{\psi}]$ through the saddle point method, Düring et al. succeeded in obtaining the following macroscopic recursive equations for the order parameters of (8)–(10).

$$m(s) = \left\langle \xi^s \int \{d\boldsymbol{v}d\boldsymbol{w}\}\, e^{i\boldsymbol{v}\cdot\boldsymbol{w}-\frac{1}{2}\boldsymbol{w}\cdot\boldsymbol{R}\boldsymbol{w}} \tanh\beta\left[\xi^s m(s-1) + \theta(s-1) + \sqrt{\alpha}v(s-1)\right] \right\rangle_\xi, \tag{11}$$

$$\begin{aligned} G(s, s') = \delta_{s,s'+1}\beta\Bigg\{ 1 - \Bigg\langle \int \{d\boldsymbol{v}d\boldsymbol{w}\}\, e^{i\boldsymbol{v}\cdot\boldsymbol{w}-\frac{1}{2}\boldsymbol{w}\cdot\boldsymbol{R}\boldsymbol{w}} \\ \times \tanh^2\beta\left[\xi^s m(s-1) + \theta(s-1) + \sqrt{\alpha}v(s-1)\right] \Bigg\rangle_\xi \Bigg\}, \end{aligned} \tag{12}$$

$$\begin{aligned} C(s, s') = \delta_{s,s'} + (1 - \delta_{s,s'})\Bigg\langle \int \{d\boldsymbol{v}d\boldsymbol{w}\}\, e^{i\boldsymbol{v}\cdot\boldsymbol{w}-\frac{1}{2}\boldsymbol{w}\cdot\boldsymbol{R}\boldsymbol{w}} \\ \times \tanh\beta\left[\xi^s m(s-1) + \theta(s-1) + \sqrt{\alpha}v(s-1)\right] \\ \times \tanh\beta\left[\xi^{s'} m(s'-1) + \theta(s'-1) + \sqrt{\alpha}v(s'-1)\right] \Bigg\rangle_\xi, \end{aligned} \tag{13}$$

where $\{d\boldsymbol{v}d\boldsymbol{w}\} = \prod_{s<t}\left[\frac{dv(s)}{\sqrt{2\pi}} \frac{dw(s)}{\sqrt{2\pi}}\right]$ for $\boldsymbol{v} = (v(0), v(1), \cdots, v(t-1))^T$, $\boldsymbol{w} = (w(0), w(1), \cdots, w(t-1))^T$, $\langle \cdot \rangle_\xi$ denotes the average over all ξ's, and the matrix $\boldsymbol{R}$ is given

by

$$\boldsymbol{R} = \sum_{n \geq 0} \left[(\boldsymbol{G})^n \, \boldsymbol{C} \left(\boldsymbol{G}^\dagger \right)^n \right]. \tag{14}$$

IV. DYNAMIC TREATMENT OF THE PATH-INTEGRAL METHOD

A. Transient dynamics

These formal dynamical equations seem to be intractable because the numerical complexity in directly calculating these equations becomes exponentially large with respect to the time s. Although the rigorous solution of these equations formally has an ability to treat the macroscopic state transition, Düring et al. derived stationary state equations from these formal dynamical equations, and only analyzed the stationary properties of the storage capacity and the phase diagram. In contrast, we have succeeded in obtaining a tractable description of the macroscopic dynamic state transition from the result as shown below.

Since the matrix $\boldsymbol{R}$ is $R(s, s') = \langle v(s)v(s') \rangle$, the matrix $\boldsymbol{R}$ represents the covariance matrix of crosstalk noise $\boldsymbol{v}$. We need the value of $R(s, s')$ for each time to analyze the transient dynamics exactly. In consideration of this, we reconsidered (12) and succeeded in deriving a recurrence relation form of $R(s, s')$. From (12), $G(s, s') = 0$ is satisfied when $s \neq s' + 1$. Therefore, the matrix $\boldsymbol{G}$ can be given by

$$\boldsymbol{G} = \begin{bmatrix} 0 & 0 & 0 & \cdots & 0 \\ g_1 & 0 & 0 & \cdots & 0 \\ 0 & g_2 & 0 & \cdots & 0 \\ \vdots & & \ddots & & \vdots \\ 0 & \cdots & 0 & g_{t-1} & 0 \end{bmatrix}, \tag{15}$$

with $g_s = G(s, s-1)$. From this, we can easily find that $G^n(s, s') = \delta_{s, s'+n} \prod_{\tau=0}^{n-1} g_{s-\tau}, (n \geq 1)$ and

$$\left[(\boldsymbol{G})^n \, \boldsymbol{C} \left(\boldsymbol{G}^\dagger \right)^n \right] (s, s') = \begin{cases} C(s, s') & , n = 0 \\ C(s-n, s'-n) \prod_{\tau=0}^{n-1} g_{s-\tau} \prod_{\tau'=0}^{n-1} g_{s'-\tau'} & , 1 \leq n \leq s \\ 0 & , n > s \end{cases} \tag{16}$$

From (14), $R(s, s')$ can be reduced to

$$R(s, s') = C(s, s') + \sum_{n \geq 1}^{s} C(s-n, s'-n) \prod_{\tau=0}^{n-1} G(s-\tau, s-\tau-1) \prod_{\tau'=0}^{n-1} G(s'-\tau', s'-\tau'-1)$$

6

$$\tag{17}$$

$$= C(s, s') + C(s-1, s'-1)G(s, s-1)G(s', s'-1)$$

$$+ \sum_{n \geq 1}^{s-1} C(s-n-1, s'-n-1) \prod_{\tau=0}^{n} G(s-\tau, s-\tau-1) \prod_{\tau'=0}^{n} G(s'-\tau', s'-\tau'-1) \tag{18}$$

$$= C(s, s') + G(s, s-1)G(s', s'-1) \left\{ C(s-1, s'-1) + \sum_{n \geq 1}^{s-1} C(s-n-1, s'-n-1) \right.$$

$$\left. \times \prod_{\tau=0}^{n-1} G(s-\tau-1, s-\tau-2) \prod_{\tau'=0}^{n-1} G(s'-\tau'-1, s'-\tau'-2) \right\} \tag{19}$$

We can therefore derive a recurrence relation form of $R(s, s')$:

$$R(s, s') = C(s, s') + G(s, s-1)G(s', s'-1)R(s-1, s'-1). \tag{20}$$

Using this recurrence relation, we can evaluate the value of $R(s, s')$ for each time.

Next, since the terms $\tanh(\cdot)$ of $m(s)$ and $G(s, s-1)$ include only the variable $v(s-1)$, these multiple integral equations can be reduced to the following single integral equations by using (A18) in the AppendixA.

$$m(s) = \left\langle \xi^s \int Dz \tanh \beta \left[\xi^s m(s-1) + \theta(s-1) + z\sqrt{\alpha R(s-1, s-1)} \right] \right\rangle_\xi \tag{21}$$

$$G(s, s-1) = \beta \left\{ 1 - \left\langle \int Dz \tanh^2 \beta \left[\xi^s m(s-1) + \theta(s-1) + z\sqrt{\alpha R(s-1, s-1)} \right] \right\rangle_\xi \right\}, \tag{22}$$

with the familiar abbreviation $Dz = \frac{dz}{\sqrt{2\pi}} e^{-\frac{1}{2}z^2}$. Since $C(s, s')$ includes $v(s-1)$ and $v(s'-1)$, $C(s, s')$ can be reduced to a double integral equation from (A18),

$$C(s, s) = 1 \tag{23}$$

$$C(s, 0) = \left\langle \xi^p m(0) \int Dz \tanh \beta \left[\xi^s m(s-1) + \theta(s-1) + z\sqrt{\alpha R(s-1, s-1)} \right] \right\rangle_\xi \tag{24}$$

$$= 0 \tag{25}$$

$$C(s, s') = \left\langle \int \frac{dz e^{-\frac{1}{2} z \cdot R_{11}^{-1} z}}{2\pi |R_{11}|^{\frac{1}{2}}} \tanh \beta \left[\xi^s m(s-1) + \theta(s-1) + \sqrt{\alpha} z(s-1) \right] \right.$$

$$\left. \times \tanh \beta \left[\xi^{s'} m(s'-1) + \theta(s'-1) + \sqrt{\alpha} z(s'-1) \right] \right\rangle_\xi \tag{26}$$

where the matrix R_{11} is a 2×2 matrix consisting of the elements of R at time $s-1$ and time $s'-1$, and $z = [z(s-1), z(s'-1)]^T$. We therefore have the macroscopic state equations (20)–(26) for each time, and can analyze the transient dynamics exactly.

7

B.   Stationary state equations

Let us derive stationary state equations from our macroscopic state equations. We assume $m(t) \to m$ and $R(t, t') \to r$ when $t, t' \to \infty$. In this case, we can get

$$m = \left\langle \xi \int Dz \tanh \beta \left[\xi m + \theta + z\sqrt{\alpha r} \right] \right\rangle_{\xi}, \tag{27}$$

$$q = \left\langle \int Dz \tanh^2 \beta \left[\xi m + \theta + z\sqrt{\alpha r} \right] \right\rangle_{\xi}, \tag{28}$$

and also $G(t, t-1) \to \beta (1 - q)$. We can, therefore, obtain

$$r = \frac{1}{1 - \beta^2 (1 - q)^2}. \tag{29}$$

These equations (27)–(29) are coincident with those obtained by Düring el al. Using (27)–(29), the stationary state can be evaluated.

V.   STATISTICAL NEURODYNAMICS

A.   Finite temperature case

Macroscopic state equations have also been derived for a sequential associative memory model with absolute zero temperature $T = 0$ by the statistical neurodynamics [25]. In this paper, we derive the macroscopic state equations for the present model with finite temperature $T \geq 0$, by the statistical neurodynamics [20]. In the statistical neurodynamics, the input is divided into a signal term and a crosstalk noise term. From (2) and (4), we obtain

$$h_i(s) = \xi_i^{s+1} m^s(s) + z_i(s) + \theta_i(s), \tag{30}$$

$$z_i(s) = \sum_{\mu \neq s}^{p} \xi_i^{\mu+1} m^{\mu}(s), \tag{31}$$

$$m^{\mu}(s) = \frac{1}{N} \sum_i \xi_i^{\mu} \sigma_i(s). \tag{32}$$

The overlaps $m^{\mu}(s)$ are defined for each pattern $\boldsymbol{\xi}^{\mu}$. We assume that the crosstalk noise $z_i(s)$ is normally distributed with mean 0 and variance $\rho^2(s, s)$. Then, the sequence overlap $m(s) = m^s(s)$ for condensed patterns becomes

$$m(s) = \left\langle \xi^s \int Dz \tanh \beta \left[\xi^s m(s-1) + \theta(s-1) + z\rho(s-1, s-1) \right] \right\rangle_{\xi}. \tag{33}$$

8

Next, let us evaluate the overlap $m^\mu(s), \mu \neq s$ between the network state $\boldsymbol{\sigma}(s)$ and the uncondensed pattern $\boldsymbol{\xi}^\mu$ in order to calculate the covariance matrix $\rho^2(s, s') = E\left[z_i(s)z_i(s')\right]$ of the crosstalk noise of (31). We assume that the pattern ξ_i^μ and the state $\sigma_i(s)$ are independent regarding i. The state $\sigma_i(s)$ is correlated with the uncondensed pattern ξ_i^μ, because the local field $h_i(s-1)$ includes the pattern $\boldsymbol{\xi}^\mu$. From (30), since the overlap $m^\mu(s)$ is $O(1/\sqrt{N})$, the term $\tanh\left[\beta h_i(s-1)\right]$, which determines the state $\sigma_i(s)$ stochastically, is expanded as follows:

$$\tanh\left[\beta h_i(s-1)\right] = \tanh\left[\beta h_i^{(\mu)}(s-1)\right] + \beta \xi_i^\mu m^{\mu-1}(s-1)\operatorname{sech}^2\left[\beta h_i^{(\mu)}(s-1)\right], \quad (34)$$

$$h_i^{(\mu)}(s-1) = \xi_i^s m^{s-1}(s-1) + \frac{1}{N}\sum_{\nu\neq s,\mu-1}^p \xi_i^{\nu+1} m^\nu(s-1) + \theta_i(s-1). \quad (35)$$

Here, we use $(\tanh x)' = 1 - \tanh^2 x = \operatorname{sech}^2 x$. Then, we get

$$\begin{aligned}\operatorname{Prob}\left[\sigma_i(s)|h_i(s-1)\right] &= \operatorname{Prob}\left[\sigma_i(s)|h_i^{(\mu)}(s-1)\right] \\ &\quad + \frac{1}{2}\left[1 + \beta\xi_i^\mu\sigma_i(s)m^{\mu-1}(s-1)\operatorname{sech}^2\beta h_i^{(\mu)}(s-1)\right]. \quad (36)\end{aligned}$$

We can derive

$$m^\mu(s) = \frac{1}{N}\sum_i \xi_i^\mu \sigma_i^{(\mu)}(s) + U(s)m^{\mu-1}(s-1). \quad (37)$$

Note that $\sigma_i^{(\mu)}(s)$ is independent of ξ_i^μ, and $U(s)$ is given by

$$U(s) = \beta\left\langle\int Dz\,\operatorname{sech}^2\beta\left[\xi^s m(s-1) + \theta(s-1) + z\rho(s-1)\right]\right\rangle_\xi \quad (38)$$

$$= \beta\left\{1 - \left\langle\int Dz\,\tanh^2\beta\left[\xi^s m(s-1) + \theta(s-1) + z\rho(s-1)\right]\right\rangle_\xi\right\}. \quad (39)$$

Therefore, the covariance of the crosstalk noise is given by

$$\begin{aligned}\rho^2(s, s') &= \alpha E\left[\frac{1}{N}\sum_{i=1}^N \sigma_i^{(\mu)}(s)\sigma_i^{(\mu)}(s')\right] + U(s)U(s')E\left[\sum_{\mu\neq s,s'}^p m^{\mu-1}(s-1)m^{\mu-1}(s'-1)\right] \\ &\quad + U(s')E\left[\frac{1}{N}\sum_{\mu\neq s,s'}^p\sum_i \xi_i^\mu\sigma_i^{(\mu)}(s)m^{\mu-1}(s'-1)\right] \\ &\quad + U(s)E\left[\frac{1}{N}\sum_{\mu\neq s,s'}^p\sum_i \xi_i^\mu\sigma_i^{(\mu)}(s')m^{\mu-1}(s-1)\right]. \quad (40)\end{aligned}$$

From (37), the third term on the RHS of (40) becomes

$$U(s')E\left[\frac{1}{N}\sum_{\mu\neq s,s'}^p\sum_i \xi_i^\mu\sigma_i^{(\mu)}(s)m^{\mu-1}(s'-1)\right]$$

$$= U(s')E\left[\frac{1}{N^2}\sum_{\mu\neq s,s'}^{p}\sum_{i}\xi_i^{\mu}\xi_i^{\mu-1}\sigma_i^{(\mu)}(s)\sigma_i^{(\mu-1)}(s'-1)\right]$$

$$+U(s')U(s'-1)E\left[\frac{1}{N}\sum_{\mu\neq s,s'}^{p}\sum_{i}\xi_i^{\mu}\sigma_i^{(\mu)}(s)m^{\mu-2}(s'-2)\right]. \tag{41}$$

According to the literature [24], (41) becomes zero as follows. Since ξ_i^{μ} and $\xi_i^{\mu-1}$ are independent of $\sigma_i^{(\mu)}(s)$ and $\sigma_i^{(\mu-1)}(s'-1)$, respectively, the first term on the RHS of (41) becomes $E\left[\xi_i^{\mu}\xi_i^{\mu-1}\sigma_i^{(\mu)}(s)\sigma_i^{(\mu-1)}(s'-1)\right]=0$. Using (37) to (41) up to the initial time iteratively, (41) becomes

$$U(s')E\left[\frac{1}{N}\sum_{\mu\neq s,s'}^{p}\sum_{i}\xi_i^{\mu}\sigma_i^{(\mu)}(s)m^{\mu-1}(s'-1)\right] = \prod_{\tau=1}^{s'}U(\tau)E\left[\frac{1}{N}\sum_{\mu\neq s,s'}^{p}\sum_{i}\xi_i^{\mu}\sigma_i^{(\mu)}(s)m^{\mu-s'}(0)\right]. \tag{42}$$

Because of the sequential associative memory with $p = \alpha N$ period, the correlations for $s' = p, 2p, 3p\cdots$ remain. These can however be neglected in the limit $N \to \infty$. Therefore, the third term on the RHS of (40) becomes zero. Similarly, the forth term also becomes zero. Finally, the covariance can be given by

$$\rho^2(s, s') = \alpha C(s, s') + U(s)U(s')\rho^2(s - 1, s' - 1). \tag{43}$$

B. Path-integral method and statistical neurodynamics

Let us compare the results obtained by the path-integral method and the results obtained by the statistical neurodynamics. From (20) and (43), let $\rho^2(s, s')$ correspond to $\alpha R(s, s')$. In this case, we obtain $U(s) = G(s, s-1)$ from (22) and (39), and then $\rho^2(s, s') = \alpha R(s, s')$ from (20) and (43). Moreover, the overlap from (21) is equal to one from (33).

As stated above, both theories give the same macroscopic state equations for the sequential associative memory model. This finding means that the crosstalk noise in the present model is normally distributed even if the network fails in retrieval, and also that the macroscopic state equations obtained by the statistical neurodynamics can give the exact solution.

VI. RETRIEVAL PROCESS

In this section, let us discuss the transient dynamics of the sequential associative memory model. Since macroscopic state equations obtained by the statistical neurodynamics are equivalent to those by the path-integral method, we use the notations of $m(t), U(t)$, and $\rho^2(t, t')$. Let $\rho^2(t, t)$ be $\rho^2(t, t) = \alpha r(t)$ when $t' = t$. We analyze the case of $\theta(t) = 0$ and derive the macroscopic state equations,

$$m(t+1) = \left\langle \xi^{t+1} \int Dz \tanh \beta \left[\xi^{t+1} m(t) + z\sqrt{\alpha r(t)} \right] \right\rangle_\xi \tag{44}$$

$$U(t+1) = \beta \left\{ 1 - \left\langle \int Dz \tanh^2 \beta \left[\xi^{t+1} m(t) + z\sqrt{\alpha r(t)} \right] \right\rangle_\xi \right\}, \tag{45}$$

$$r(t+1) = 1 + U^2(t+1)r(t). \tag{46}$$

Figure 1 shows the time evolution of the overlap $m(t)$. The solid lines represent results obtained by the macroscopic state equations (44)–(46), and the broken lines represent results obtained by computer simulations with $N = 100000$, where the loading rate is $\alpha = 0.20, 0.26$ and the inverse temperature is $\beta = 5$ ($T = 0.2$). The abscissa denotes the time t, and the ordinate denotes the overlap $m(t)$. In this case, the storage capacity is $\alpha_c = 0.246$. As shown in Fig. 1, our theory can describe the transient dynamics quantitatively even if the network fails in retrieval or the loading rate α exceeds the storage capacity α_c.

In the autoassociative memory models, the crosstalk noise is not normally distributed when the network fails in retrieval [20, 23]. In the present sequential associative memory model, however, the macroscopic state equations obtained by the path-integral method are represented in the form of a single or double Gaussian integral. Therefore, the first, second, third, and fourth cumulants $C_1(t), C_2(t), C_3(t), C_4(t)$ are evaluated in order to verify the distribution of the crosstalk noise. When the crosstalk noise is normally distributed, the third and fourth cumulants are zero. The cumulants are defined by

$$C_1(t) = \overline{z}(t), \tag{47}$$

$$C_2(t) = \overline{z^2}(t) - \overline{z}^2(t), \tag{48}$$

$$C_3(t) = \overline{z^3}(t) - 3\overline{z}(t)\overline{z^2}(t) + 2\overline{z}^3(t), \tag{49}$$

$$C_4(t) = \overline{z^4}(t) - 3\left(\overline{z^2}(t)\right)^2 - 4\overline{z}(t)\overline{z^3}(t) + 12\overline{z}^2(t)\overline{z^2}(t) - 6\overline{z}^4(t), \tag{50}$$

where $\overline{z^n}(t)$ denotes the nth-order moment for the crosstalk noise $z_i(t)$ and is defined as

$$\overline{z^n}(t) = \frac{1}{N} \sum_{i=1}^{N} \{z_i(t)\}^n . \tag{51}$$

The cumulants $C_1(t)$ and $C_2(t)$ represent the average and variance of $z(t)$, respectively.

Figure 2 shows the time evolution of cumulants and overlap $m(t)$, where the loading rate is $\alpha = 0.20, 0.26$ and the inverse temperature is $\beta = 5$ ($T = 0.2$). The initial overlap is $m(0) = 0.2$, where the network fails in retrieval. The solid lines represent the overlap $m(t)$ and the variance of the crosstalk noise $r(t)$ obtained by our theory. These lines agree with the overlap and the cumulant $C_2(t)$ obtained by the computer simulations. Since the third and fourth cumulants are zero, we can find that the crosstalk noise is normally distributed. In the sequential associative memory model, the third and fourth cumulants hold $C_3(t) = C_4(t) = 0$, as obtained by the path-integral method, even if the network fails in retrieval. The Figure 2 shows that the Gaussian assumption in the statistical neurodynamics folds for the present model.

Figure 3 shows the transition of the overlap $m(t)$ and the variance of the crosstalk noise $\alpha r(t)$. The solid lines represent results obtained by our theory and the broken lines represent results obtained by computer simulations with $N = 100000$. The loading rate is $\alpha = 0.20$ and the inverse temperature is $\beta = 5$ ($T = 0.2$). As shown in Fig. 3, there are two stable stationary states; one is $m \approx 1$, which represents a retrieval state, and the other is $m = 0$, which represents a non-retrieval state. We can therefore define the critical overlap, which determines whether patterns will be retrieved. When the initial overlap is larger than the critical overlap m_c, stored patterns can be retrieved. Namely, as shown in Fig. 3, there is a separatrix on the locus starting from the initial overlap m_c, and the network passes through the separatrix at time $t = 1$. In general, an unstable stationary state obtained by macroscopic state equations does not agree with a separatrix obtained by microscopic dynamics, e.g., (1). As shown by the cross mark in Fig. 3, however, we can find that the unstable stationary state agrees with the separatrix for the present model.

Figure 4 shows a basin of attraction where the inverse temperature is $\beta = 5$. The abscissa denotes the loading rate α, and the ordinate denotes the overlap. The solid line represents a result obtained by theory. The lower line represents the critical overlap m_c, and the upper line represents the stationary overlap m_∞ at time $t \to \infty$, where the network starts from the initial overlap $m(0) = 1$. The intersection between the critical overlap m_c and the stationary

overlap m_∞ gives the storage capacity α_c. The broken lines represent the overlap m, which is the unstable stationary state given by equations (27)–(29). The error bars represent the median, and the first and third quartiles over 11 trials of the overlaps m_c and m_∞, which are obtained by computer simulations with $N = 10000$. As shown in this figure, the basin of attraction obtained by the theory quantitatively coincides with that of the computer simulations.

VII. CONCLUSIONS

We rigorously derived dynamic macroscopic state equations for the sequential associative memory model through the path-integral method. This suggested that the crosstalk noise is normally distributed for the sequential associative memory model. We also examined the cumulants of the crosstalk noise by computer simulations, and found the third and fourth cumulants to be zero. This finding strongly supported the normally distributed crosstalk noise. Using this exact solution, we obtained dynamical properties such as the critical overlap m_c, the temporal behavior of the overlap, and so on. These theoretically obtained results agreed with those of computer simulations. We also found that the separatrix coincides with the unstable fixed point of the macroscopic stationary state equations.

Historically, dynamic macroscopic state equations have been derived by the statistical neurodynamics for a sequential associative memory model with zero temperature $T = 0$ assuming the crosstalk noise to obey the Gaussian distribution [25]. We extended this theory to the finite temperature case, and compared dynamic macroscopic state equations by the statistical neurodynamics with those by the path-integral method. As a result, we found both to be completely equivalent for the sequential associative memory model. This means that the statistical neurodynamics is exact for the sequential associative memory model.

For the sequential associative memory model, we could drive the recurrence relation of $R(s, s')$ and the dynamic macroscopic state equations. This is the reason why no effective self-interaction, which is caused by the time correlation of states, remains. In contrast, since only one pattern is retrieved for an autoassociative memory model, the effect of the intrinsic time correlation can not be avoided and the distribution of the crosstalk noise becomes non-Gaussian. It is known that this treatment of the autoassociative memory model is

13

intractable [9, 26].

APPENDIX A: MULTIPLE GAUSSIAN INTEGRAL

In order to calculate equations (11) to (13), it is sufficient to treat the following form of a multiple Gaussian integral,

$$\int \{d\boldsymbol{v} d\boldsymbol{w}\}\, e^{i\boldsymbol{v}\cdot\boldsymbol{w}-\frac{1}{2}\boldsymbol{w}\cdot\boldsymbol{R}\boldsymbol{w}} f(\boldsymbol{v}_1)\,, \tag{A1}$$

where we put $\boldsymbol{v} = (\boldsymbol{v}_1, \boldsymbol{v}_2)^T$. We define $\boldsymbol{S}$ as the inverse matrix of $\boldsymbol{R}$. Corresponding to the representation of $\boldsymbol{v} = (\boldsymbol{v}_1, \boldsymbol{v}_2)^T$, the matrix $\boldsymbol{R}$ and its inversion $\boldsymbol{S}$ are represented as,

$$\boldsymbol{R} = \begin{pmatrix} \boldsymbol{R}_{11} & \boldsymbol{R}_{12} \\ \boldsymbol{R}_{21} & \boldsymbol{R}_{22} \end{pmatrix}, \qquad \boldsymbol{S} = \begin{pmatrix} \boldsymbol{S}_{11} & \boldsymbol{S}_{12} \\ \boldsymbol{S}_{21} & \boldsymbol{S}_{22} \end{pmatrix}. \tag{A2}$$

For example, $\boldsymbol{v}_1$ and $\boldsymbol{R}_{11}$ are $v(s-1)$ and $R(s-1, s-1)$ with equations (11) and (12), respectively, while $\boldsymbol{v}_1 = (v(s-1), v(s'-1))^T$ and

$$\boldsymbol{R}_{11} = \begin{pmatrix} R(s-1, s-1) & R(s-1, s'-1) \\ R(s'-1, s-1) & R(s'-1, s'-1) \end{pmatrix}, \tag{A3}$$

with equation (13). According to the definition, $\boldsymbol{S}\boldsymbol{R} = \boldsymbol{I}$. We obtain

$$\boldsymbol{S}_{11}\boldsymbol{R}_{11} + \boldsymbol{S}_{12}\boldsymbol{R}_{21} = \boldsymbol{I} \tag{A4}$$

$$\boldsymbol{S}_{21}\boldsymbol{R}_{11} + \boldsymbol{S}_{22}\boldsymbol{R}_{21} = \boldsymbol{0}, \tag{A5}$$

where $\boldsymbol{I}$ and $\boldsymbol{0}$ are the identity and zero matrix, respectively. Solving (A4) and (A5) with respect to $\boldsymbol{R}_{11}$, we obtain $\boldsymbol{R}_{11} = \left(\boldsymbol{S}_{11} - \boldsymbol{S}_{12}\boldsymbol{S}_{22}^{-1}\boldsymbol{S}_{21}\right)^{-1}$.

Accordingly, the integral of equation (A1) is obtained as,

$$\int \{d\boldsymbol{v} d\boldsymbol{w}\}\, e^{i\boldsymbol{v}\cdot\boldsymbol{w}-\frac{1}{2}\boldsymbol{w}\cdot\boldsymbol{R}\boldsymbol{w}} f(\boldsymbol{v}_1) \tag{A6}$$

$$= \int \{d\boldsymbol{v} d\boldsymbol{w}\}\, e^{-\frac{1}{2}\left(\boldsymbol{w}-i\boldsymbol{R}^{-1}\boldsymbol{v}\right)^{\dagger}\boldsymbol{R}\left(\boldsymbol{w}-i\boldsymbol{R}^{-1}\boldsymbol{v}\right)-\frac{1}{2}\boldsymbol{v}\cdot\boldsymbol{R}^{-1}\boldsymbol{v}} f(\boldsymbol{v}_1) \tag{A7}$$

$$= \frac{1}{|\boldsymbol{R}|^{\frac{1}{2}}} \int \{d\boldsymbol{v}\}\, e^{-\frac{1}{2}\boldsymbol{v}\cdot\boldsymbol{R}^{-1}\boldsymbol{v}} f(\boldsymbol{v}_1) \tag{A8}$$

$$= \frac{1}{|\boldsymbol{R}|^{\frac{1}{2}}} \int \{d\boldsymbol{v}\}\, e^{-\frac{1}{2}\left(\boldsymbol{v}_1\cdot\boldsymbol{S}_{11}\boldsymbol{v}_1+\boldsymbol{v}_1\cdot\boldsymbol{S}_{12}\boldsymbol{v}_2+\boldsymbol{v}_2\cdot\boldsymbol{S}_{21}\boldsymbol{v}_1+\boldsymbol{v}_2\cdot\boldsymbol{S}_{22}\boldsymbol{v}_2\right)} f(\boldsymbol{v}_1) \tag{A9}$$

$$= \frac{1}{|\boldsymbol{R}|^{\frac{1}{2}}} \int \{d\boldsymbol{v}\}\, e^{-\frac{1}{2}\left(\boldsymbol{v}_2+\boldsymbol{S}_{22}^{-1}\boldsymbol{S}_{12}^{\dagger}\boldsymbol{v}_1\right)^{\dagger}\boldsymbol{S}_{22}\left(\boldsymbol{v}_2+\boldsymbol{S}_{22}^{-1}\boldsymbol{S}_{21}\boldsymbol{v}_1\right)-\frac{1}{2}\boldsymbol{v}_1^{\dagger}\left(\boldsymbol{S}_{11}-\boldsymbol{S}_{12}\boldsymbol{S}_{22}^{-1}\boldsymbol{S}_{21}\right)\boldsymbol{v}_1} f(\boldsymbol{v}_1)$$

14

$$\tag{A10}$$

$$= \frac{1}{|\boldsymbol{R}|^{\frac{1}{2}}|\boldsymbol{S}_{22}|^{\frac{1}{2}}} \int \{d\boldsymbol{v}_1\} \, e^{-\frac{1}{2}\boldsymbol{v}_1 \cdot \boldsymbol{R}_{11}^{-1}\boldsymbol{v}_1} f(\boldsymbol{v}_1), \tag{A11}$$

with $\{d\boldsymbol{v}\} = \prod_{s<t} \left[\frac{dv(s)}{\sqrt{2\pi}} \right]$ for $\boldsymbol{v} = (v(0), v(1), \cdots, v(t-1))^T$, and $\{d\boldsymbol{v}_1\} = \frac{dv(s-1)}{\sqrt{2\pi}}$ or $\{d\boldsymbol{v}_1\} = \frac{dv(s-1)}{\sqrt{2\pi}}\frac{dv(s'-1)}{\sqrt{2\pi}}$. Substituting the following identities,

$$|\boldsymbol{S}| = \begin{vmatrix} \boldsymbol{S}_{11} - \boldsymbol{S}_{12}\boldsymbol{S}_{22}^{-1}\boldsymbol{S}_{21} & \boldsymbol{0} \\ \boldsymbol{S}_{21} & \boldsymbol{S}_{22} \end{vmatrix} \tag{A12}$$

$$= |\boldsymbol{S}_{11} - \boldsymbol{S}_{12}\boldsymbol{S}_{22}^{-1}\boldsymbol{S}_{21}||\boldsymbol{S}_{22}| \tag{A13}$$

$$|\boldsymbol{S}||\boldsymbol{R}| = 1, \tag{A14}$$

into equation (A11), we get

$$\frac{1}{|\boldsymbol{R}|^{\frac{1}{2}}|\boldsymbol{S}_{22}|^{\frac{1}{2}}} \int \{d\boldsymbol{v}_1\} \, e^{-\frac{1}{2}\boldsymbol{v}_1 \cdot \boldsymbol{R}_{11}^{-1}\boldsymbol{v}_1} f(\boldsymbol{v}_1) \tag{A15}$$

$$= |\boldsymbol{S}_{11} - \boldsymbol{S}_{12}\boldsymbol{S}_{22}^{-1}\boldsymbol{S}_{21}|^{\frac{1}{2}} \int \{d\boldsymbol{v}_1\} \, e^{-\frac{1}{2}\boldsymbol{v}_1 \cdot \boldsymbol{R}_{11}^{-1}\boldsymbol{v}_1} f(\boldsymbol{v}_1) \tag{A16}$$

$$= \frac{1}{|\boldsymbol{R}_{11}|^{\frac{1}{2}}} \int \{d\boldsymbol{v}_1\} \, e^{-\frac{1}{2}\boldsymbol{v}_1 \cdot \boldsymbol{R}_{11}^{-1}\boldsymbol{v}_1} f(\boldsymbol{v}_1). \tag{A17}$$

We can therefore obtain a simple form of the multiple integral,

$$\int \{d\boldsymbol{v}d\boldsymbol{w}\} \, e^{i\boldsymbol{v}\cdot\boldsymbol{w} - \frac{1}{2}\boldsymbol{w}\cdot\boldsymbol{R}\boldsymbol{w}} f(\boldsymbol{v}_1) = \frac{1}{|\boldsymbol{R}_{11}|^{\frac{1}{2}}} \int \{d\boldsymbol{v}_1\} \, e^{-\frac{1}{2}\boldsymbol{v}_1 \cdot \boldsymbol{R}_{11}^{-1}\boldsymbol{v}_1} f(\boldsymbol{v}_1). \tag{A18}$$

[1] Sourlas, N., "Spin-glass models as error-correcting codes", Nature, **339**, 693–695, 1989.

[2] Sourlas, N., "Statistical mechanics and error-correcting codes", cond-mat/9811406, 1998.

[3] Ruján, P., "Finite temperature error-correcting codes", Phys. Rev. Lett., **70**, 19, 2968–2971, 1993.

[4] Morita, T. and Tanaka, K., "Determination of parameters in an image recovery by statistical-mechanical means", Physica A, **223**, 244–262, 1996.

[5] Nishimori, H. and Wong, K. Y. M., "Statistical mechanics of image restoration and error-correcting codes", Phys. Rev. E, **60**, 1, 132–144, 1999.

[6] Iba, Y., "The Nishimori line and Bayesian statistics", J. Phys. A: Math Gen. **32**, 3875–3888, 1999.

[7] Kabashima, Y., Murayama, T., and Saad, D., "Typical performance of Gallager-type error-correcting codes", Phys. Rev. Lett., **84**, 1355–1358, 2000.

[8] Tanaka, T., "Analysis of bit error probability of direct-sequence CDMA multiuser demodulators", 14th Annual Conference on Neural Information Processing Systems (NIPS*2000), Denver, USA, 2000.

[9] Gardner, E., Derrida, B., and Mottishaw, P., "Zero temperature parallel dynamics for infinite range spin glasses and neural networks", Journal of Physique, **48**, 741–755, 1987.

[10] Amari, S. and Maginu, K., "Statistical neurodynamics of associative memory", Neural Networks, **1**, 63–73, 1988.

[11] Coolen, A. C. C. and Sherrington, D., "Dynamics of fully connected attractor neural networks near saturation", Phys. Rev. Lett., **71**, 23, 3886–3889, 1993.

[12] Hopfield, J. J., "Neural networks and physical systems with emergent collective computational abilities", Proc. Natl. Acad. Sci. USA, **79**, 2554–2558, 1982.

[13] Amit, D.J., Gutfreund, H., and Sompolinsky, H., "Information storage in neural networks with low levels of activity", Phys. Rev. A, **35**, 6, 2293–2303, 1987.

[14] Shiino, M. and Fukai, T., "Self-consistent signal-to-noise analysis and its application to analogue neural networks with asymmetric connections", J. Phys. A: Math. Gen., **25**, L375–L381, 1992.

[15] Sommers, H. J., "Path-integral approach to Ising spin-glass dynamics", Phys. Rev. Lett., **58**, 12, 1268–1271, 1987.

[16] Gomi, S. and Yonezawa, F., "A new perturbation theory for the dynamics of the Little-Hopfield model", J. Phys. A: Math. Gen., **28**, 4761–4775, 1995.

[17] Koyama, H., Fujie, N., and Seyama, H., "Results from the Gardner-Derrida-Mottishaw theory of associative memory", Neural Networks, **12**, 247–257, 1999.

[18] Düring, A., Coolen, A. C. C., and Sherrington, D., "Phase diagram and storage capacity of sequence processing neural networks", J. Phys. A: Math Gen. **31**, 8607–8621, 1998.

[19] Patrick, A. E. and Zagrebnov, V. A., "A probabilistic approach to parallel dynamics for the Little-Hopfield model", J. Phys. A: Math. Gen, **24**, 3413–3426, 1991.

[20] Nishimori, H. and Ozeki, T., "Retrieval dynamics of associative memory of the Hopfield type", J Phys. A: Math. Gen., **26**, 859–871, 1993.

[21] Okada, M., "A hierarchy of macrodynamical equations for associative memory", Neural

Networks, **8**, 6, 833–838, 1995.

[22] Kawamura, M., Okada, M., and Hirai, Y., "Dynamics of selective recall in an associative memory model with one-to-many associations", IEEE Trans. Neural Networks, **10**, 3, 704–713, 1999.

[23] Ozeki, T. and Nishimori, H., "Noise distributions in retrieval dynamics of the Hopfield model", J Phys. A: Math. Gen., **27**, 7061–7068, 1994.

[24] Kitano, K. and Aoyagi. T., "Retrieval dynamics of neural networks for sparsely coded sequential patterns", J Phys. A: Math. Gen., **31**, L613–L620, 1998.

[25] Amari, S., "Statistical neurodynamics of various versions of correlation associative memory", Proc. IEEE Conference on Neural Networks, **1**, 633–640, 1988.

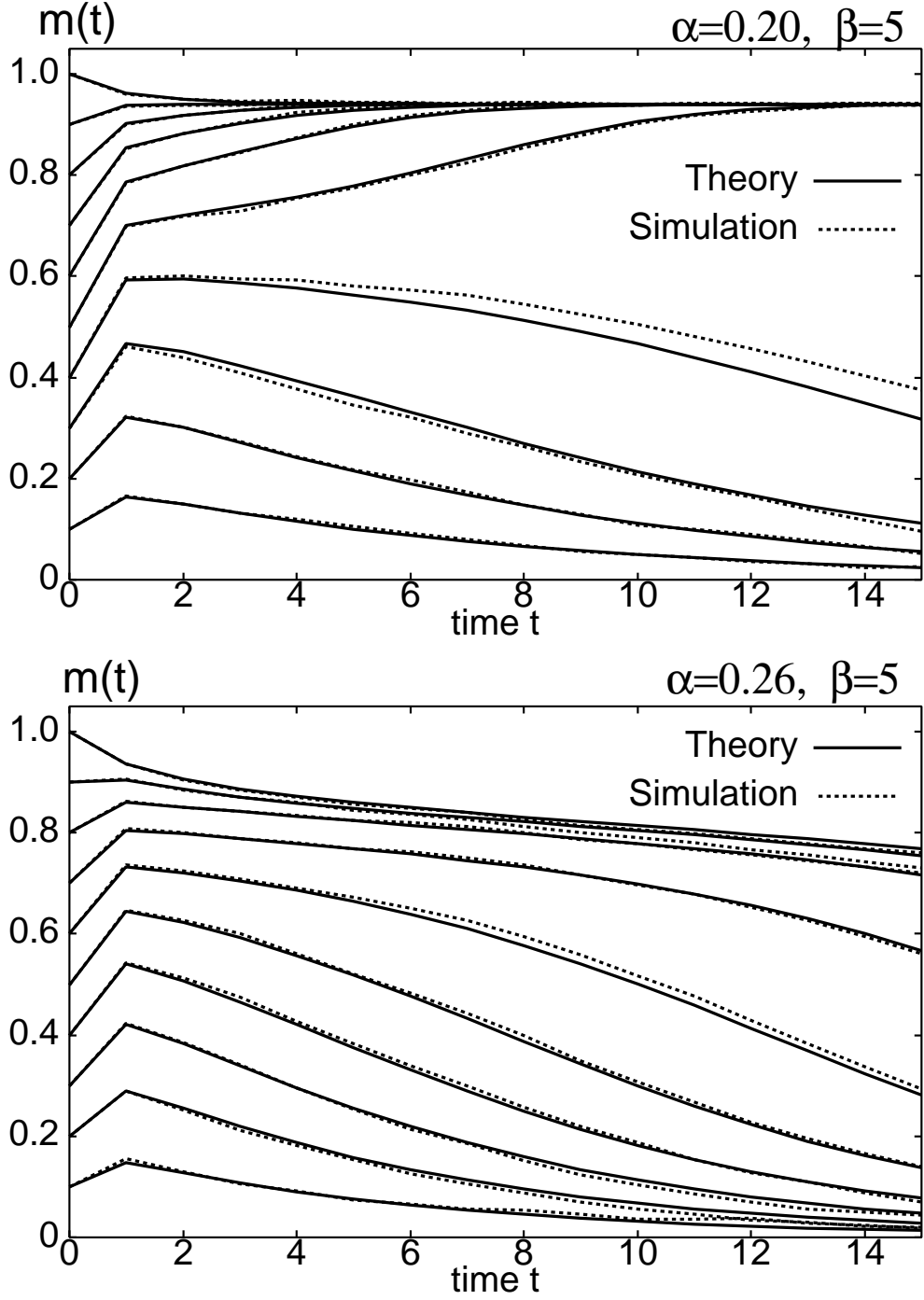[26] Coolen, A.C.C., "Statistical mechanics of recurrent neural networks II. dynamics", cond-mat/0006011, 2000.

FIG. 1: Time evolution of overlap $m(t)$ with loading rate $\alpha = 0.20, 0.26$ and inverse temperature $\beta = 5$. The solid lines denote theoretical results and the broken lines denote results by computer simulations with $N = 100000$.
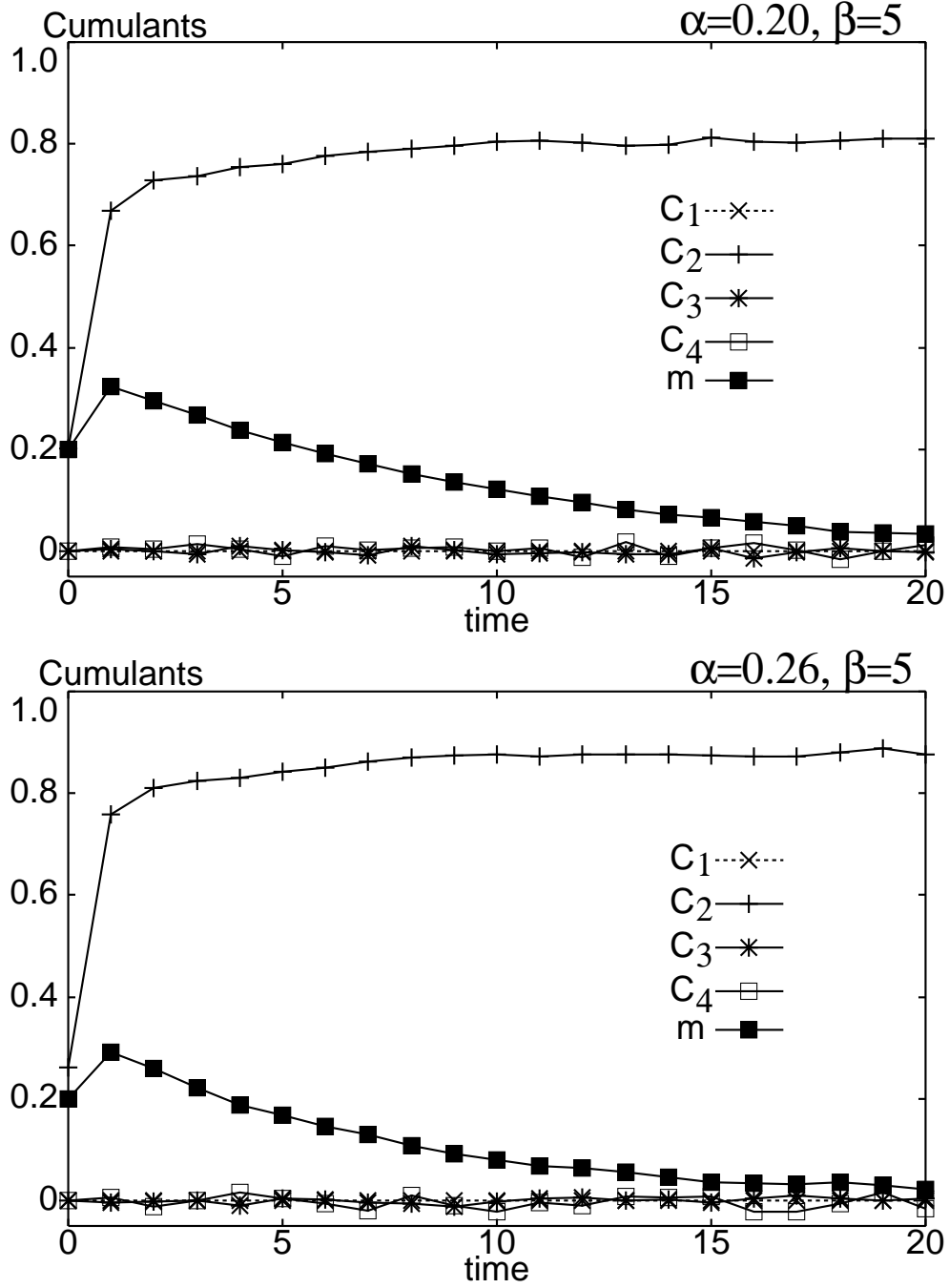
FIG. 2: Time evolution of cumulants $C_1(t), C_2(t), C_3(t), C_4(t)$ and overlap $m(t)$ with loading rate $\alpha = 0.20, 0.26$ and inverse temperature $\beta = 5$. The initial overlap is $m(0) = 0.2$. The solid lines denote theoretical results and the broken lines denote results by computer simulations with $N = 100000$.
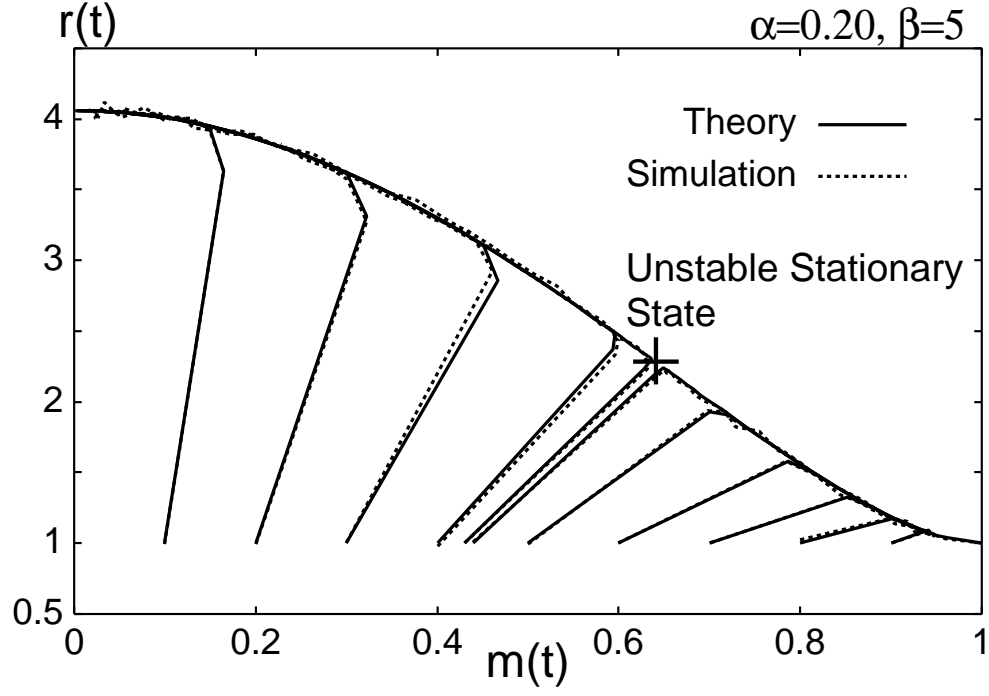
FIG. 3: Overlap $m(t)$ and variance of crosstalk noise $r(t)$ with loading rate $\alpha = 0.20$ and inverse temperature $\beta = 5$. The solid lines denote theoretical results and the broken lines denote results by computer simulations with $N = 100000$. The initial overlap is $m(0) = 0.10, \cdots, 0.40, 0.43, 0.44, 0.50, \cdots, 1.0$.
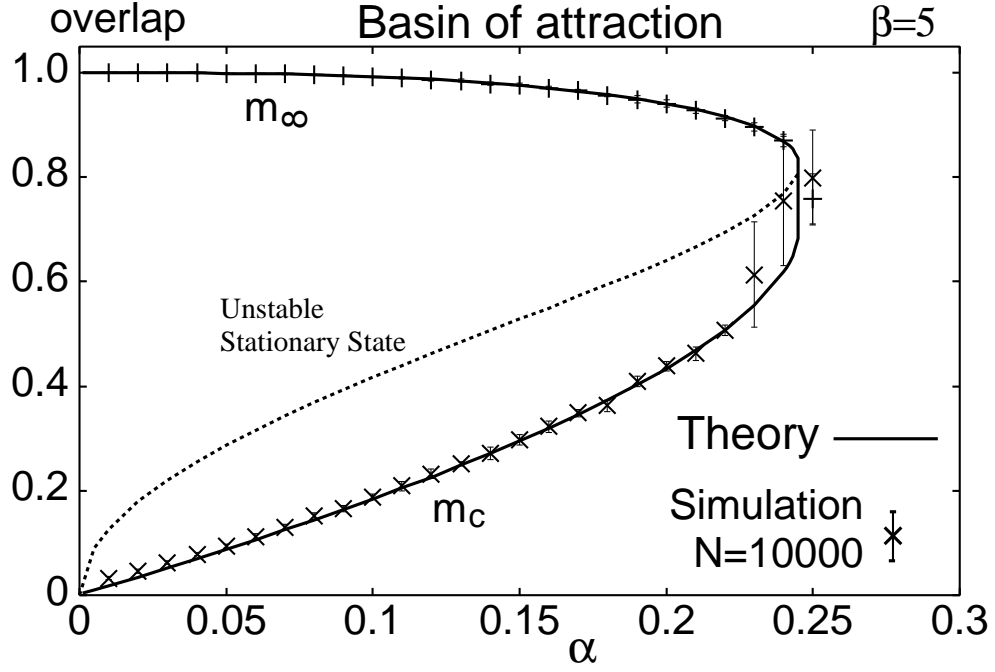
FIG. 4: Basin of attraction (solid line) obtained by theory with inverse temperature $\beta = 5$. The error bars denote the median, and first and third quartiles over 11 trials by computer simulations with $N = 10000$.